Role of Leaflet Asymmetry in the Permeability of Model Biological Membranes to Protons, Solutes, and Gases

Warren G. Hill, Rickey L. Rivers,[†] and Mark L. Zeidel

From the Laboratory of Epithelial Cell Biology, Renal-Electrolyte Division, University of Pittsburgh Medical Center, Pittsburgh, Pennsylvania 15261

abstract   Bilayer asymmetry in the apical membrane may be important to the barrier function exhibited by epithelia in the stomach, kidney, and bladder. Previously, we showed that reduced fluidity of a single bilayer leaflet reduced water permeability of the bilayer, and in this study we examine the effect of bilayer asymmetry on permeation of nonelectrolytes, gases, and protons. Bilayer asymmetry was induced in dipalmitoylphosphatidylcholine liposomes by rigidifying the outer leaflet with the rare earth metal, praseodymium (Pr^{3+}). Rigidification was demonstrated by fluorescence anisotropy over a range of temperatures from 24 to 50°C. Pr^{3+}-treatment reduced membrane fluidity at temperatures above 40°C (the phase-transition temperature). Increased fluidity exhibited by dipalmitoylphosphatidylcholine liposomes at 40°C occurred at temperatures 1–3°C higher in Pr^{3+}-treated liposomes, and for both control and Pr^{3+}-treated liposomes permeability coefficients were approximately two orders of magnitude higher at 48° than at 24°C. Reduced fluidity of one leaflet correlated with significantly reduced permeabilities to urea, glycerol, formamide, acetamide, and NH_3. Proton permeability of dipalmitoylphosphatidylcholine liposomes was only fourfold higher at 48° than at 24°C, indicating a weak dependence on membrane fluidity, and this increase was abolished by Pr^{3+}. CO_2 permeability was unaffected by temperature. We conclude: (a) that decreasing membrane fluidity in a single leaflet is sufficient to reduce overall membrane permeability to solutes and NH_3, suggesting that leaflets in a bilayer offer independent resistances to permeation, (b) bilayer asymmetry is a mechanism by which barrier epithelia can reduce permeability, and (c) CO_2 permeation through membranes occurs by a mechanism that is not dependent on fluidity.

key words: barrier function • epithelia • membrane fluidity • CO_2 • NH_3

introduction

The epithelia that line the stomach, bladder, renal collecting duct, and thick ascending limb of the nephron limit the dissipation of large proton, solute, NH_3, and CO_2 gradients by creating and maintaining a barrier to diffusion (Kikeri et al., 1989; Priver et al., 1993; Chang et al., 1994; Lande et al., 1994; Walsbren et al., 1994; Singh et al., 1995; Negrete et al., 1996a; Zeidel, 1996). The means by which they do this is not entirely clear. However, the ability of certain substances to cross biological membranes correlates well with their oil/water partition coefficient; a relationship known as Overton's Rule (Overton, 1899). This early observation has been refined into the "solubility-diffusion" model, which states that for substances to cross a lipid membrane they must partition into or dissolve in the interfacial hydrocarbon region (adjacent to head groups), and then diffuse through the membrane before reemerging on the other side (Finkelstein, 1987). Diffusion across the hydrocarbon interior is thought to occur via transport along self-propagating kinks or defects in the acyl chain packing. The rate of diffusion is therefore dependent on the thickness of the membrane, the length, saturation, and packing of the acyl chains, and the molecular volume and hydrophobicity of the solute (Walter and Gutknecht, 1986; Finkelstein, 1987; Disalvo, 1988; Paula et al., 1996). As predicted by this model, fluidity appears to be a major determinant in the rate of permeation of nonelectrolytes across lipid membranes (Worman et al., 1986; Verkman and Masur, 1988; Giocondi and Le Grimellec, 1991; Lande et al., 1995). Indeed, there is compelling experimental evidence to suggest that reducing membrane fluidity is an important means by which epithelial cells can erect barriers to permeation. The exofacial leaflet of the apical membrane is able to maintain a lipid composition that is different from that of the cytoplasmic leaflet. This is accomplished in three ways: (a) asymmetric synthesis in the Golgi and vectorial delivery of specific lipids to the exofacial leaflet (Simons and van Meer, 1988; van Meer, 1989), (b) the presence of tight junctions that isolate the apical from the basolateral plasma membrane domains (van Meer and Simons, 1986), and (c) the action of phospholipid flippases that can trans-orient phos-

---

[†]Dr. Rivers died on 19 December 1998.

Address correspondence to Mark L. Zeidel, Laboratory of Epithelial Cell Biology, Renal-Electrolyte Division, A919 Scaife Hall, 3550 Terrace St., University of Pittsburgh, Pittsburgh, PA 15261. Fax: 412-647-6222; E-mail: zeidel@med1.dept-med.pitt.edu

pholipids from one leaflet of the bilayer to the other in an energy-dependent process (Zachowski et al., 1986, 1989). The functional consequences of losing bilayer asymmetry were demonstrated when gastric apical vesicles were shown to have markedly lower water, proton, and nonelectrolyte permeabilities compared with the same membranes prepared from lipids quantitatively extracted from the vesicles and reconstituted into symmetric liposomes. (Lande et al., 1994).

Membrane permeability to a number of substances is clearly dependent on fluidity, and cells appear to limit fluidity by creating asymmetric lipid membranes at their apical pole. However, for mainly technical reasons, there have been virtually no studies undertaken to model the effects of bilayer asymmetry on permeability in artificial membranes of known composition. We have previously shown by the use of two independent methods that rigidifying a single leaflet in a bilayer reduced water permeability (Negrete et al., 1996b). In the present studies, we rigidified and thereby reduced the fluidity of the outer leaflet of dipalmitoylphosphatidylcholine (DPPC)[1] liposomes with the rare earth metal praseodymium (Pr^{3+}) (Negrete et al., 1996b). The consequences of inducing bilayer asymmetry on the permeation of solutes, gases, and protons were investigated.

materials and methods

Liposome Preparation

Powdered DPPC was obtained from Avanti Polar Lipids and suspended by vortexing (at 25 mg/ml) in buffer appropriate for the permeability to be measured. Buffers used were as follows (mM): for solutes, 150 NaCl, 10 HEPES, 20 carboxyfluorescein (CF), pH 7.5; for NH_3 and protons, 150 NaCl, 30 KCl, 10 HEPES, 0.5 CF, pH 7.5; for CO_2, 50 NaCl, 50 KCl, 20 HEPES, 0.5 CF, 0.5 mg/ml carbonic anhydrase, pH 7.4. Liposomes were prepared by probe sonication and after 90 min incubating on ice, extravesicular CF was removed by passing vesicles over a Sephadex G50 column (Sigma Chemical Co.). Vesicles were sized by quasi-elastic light scattering using a Nicomp model 270 submicron particle analyzer as described (Rivers et al., 1998). Sonication conditions (intensity and duration) were chosen that reproducibly generated vesicles with a median diameter of 110 ± 20 nm (Negrete et al., 1996b).

Solute Permeability Measurements

Permeability measurements were performed as described (Lande et al., 1995; Negrete et al., 1996b; Prasad et al., 1998; Rivers et al., 1998) using a stopped-flow fluorimeter (SF.17 MV; Applied Photophysics) with a dead time of 0.7 ms. Experiments were performed either on the same day of vesicle manufacture or the next day. Liposome size was shown not to change significantly over 24 h. To perform solute permeability measurements, liposomes were incubated in buffer containing 200 mM solute (glycerol, urea, formamide, or acetamide) for 30 min before the experiment was commenced. Any residual extravesicular CF was quenched with

_____

[1]*Abbreviations used in this paper:* CF, carboxyfluorescein; DPPC, dipalmitoylphosphatidylcholine.

anticarboxyfluorescein antibody, and then the liposomes were rapidly mixed with a solution of identical osmolality containing 100 mM solute, resulting in an extravesicular solute concentration of 150 mM. Osmolalities of all solutions were confirmed and adjusted, if necessary, by measuring freezing point depression on an Osmette A osmometer (Precision Instruments, Inc.). The applied concentration gradient results in solute efflux from liposomes followed by water efflux due to solvent drag. Vesicle shrinkage is monitored as a function of CF self-quenching. Fluorescence data from the stopped-flow fluorimeter from 6–10 individual determinations were averaged and fit to a single exponential curve using software supplied by Applied Photophysics. Solute flux across a membrane can be defined by the relation (Chang et al., 1994; Grossman et al., 1992; Lande et al., 1995):

$$J_z = dz/dt = (P_z)(SA)(\Delta C), \qquad (1)$$

where J_z is the flux and P_z is the permeability of the permeant solute z, SA is the surface area of the vesicle, and ΔC is the concentration difference of the permeant solute between the inside and outside of the vesicle. If

$$V_{rel} = V(t)/V_0, \qquad (2)$$

where V_0 is the initial volume of the vesicle and V_{rel} and $V(t)$ are the relative and absolute volumes, respectively, at time t, then for our experimental conditions:

$$dz/dt = 500(V_0 - V_0 V_{rel}) \qquad (3)$$

and

$$\Delta C = 900 - (800/V_{rel}); \qquad (4)$$

therefore,

$$dV_{rel}/dt = P_z(SA/V_0)(1/500)[(800/V_{rel}) - 900]. \qquad (5)$$

By use of parameters from the single exponential curve fit to the data, P_{solute} was solved using commercially available MathCad software (Grossman et al., 1992).

Proton Permeability

Proton permeabilities were measured using pH-dependent quenching of fluorescence as described (Rivers et al., 1998). Stopped-flow experiments were performed in which the liposomes were pretreated with 1 μM valinomycin, and then rapidly mixed with an identical buffer acidified to pH 6.50. Buffer capacity was determined on an SLM-Aminco 500C spectrofluorimeter by adding 10 mM acetate (final concentration) to liposomes as described (Rivers et al., 1998). Fluorescence data from the stopped-flow device were fit to a single exponential curve and fitting parameters were used to solve the following equation for P_{H+}:

$$J_{H+} = (P_{H+})(SA)(\Delta C) = (\Delta pH/t)(BCV), \qquad (6)$$

where J_{H+} is the flux of protons, ΔC is the initial difference in concentration of protons between the inside and outside of the vesicle, ΔpH is the change in pH when time equals τ, the time constant of the single exponential curve describing the initial change in fluorescence as a function of time, and BCV is the buffer capacity of an individual vesicle (Lande et al., 1994, 1995; Rivers et al., 1998).

NH₃ Permeability

NH_3 permeability was determined using stopped-flow fluorimetry by monitoring the pH-sensitive increase in fluorescence when vesicles equilibrated to pH 6.8 were rapidly mixed with the same buffer containing 20 mM NH_4Cl as described (Lande et al., 1994, 1995; Rivers et al., 1998). NH_3 in solution passes through the membrane and becomes protonated to NH_4^+ in the vesicle interior. By combining values for the rate of change of intravesicular pH, the final intravesicular pH, and the buffer capacity (assessed in the same way as for proton permeability), P_{NH3} was calculated (Lande et al., 1995).

CO₂ Permeability

CO_2 fluxes were determined by monitoring the pH-sensitive decrease in fluorescence when vesicles were mixed with a 100 mM $NaHCO_3/CO_2$, 20 mM HEPES, pH 7.4 buffer. CO_2 gas in the bicarbonate solution diffuses into the liposomes, whereupon it is converted to HCO_3^- and H^+ by the entrapped carbonic anhydrase. By combining values for the initial rate of change of fluorescence, the final pH, and the buffer capacity of the vesicles, P_{CO2} was calculated as described (Prasad et al., 1998).

Fluorescence Anisotropy

Membrane fluidity measurements were performed by incubating DPPC liposomes in 1 mM DPH-HPC (Molecular Probes), and then measuring anisotropy using excitation/emission wavelengths of 360 nm/430 nm on a SPEX Fluorolog 1680 double spectrometer according to standard methods (Negrete et al., 1996b). A circulating water bath allowed precise control of the temperature of the cuvette chamber, and buffer temperatures were confirmed by electronic thermometer before measurement of anisotropy. Where indicated, $PrCl_3$ was added to a final concentration of 10 mM from a 1 M stock solution.

Statistics

For all comparisons, $n = 4–6$ liposome preparations. Groups were compared using unpaired t tests. $P < 0.05$ was considered significant.

r e s u l t s

Before determining the effect of bilayer asymmetry on solute fluxes, it was necessary to ensure that the solute was not altering the ability of Pr^{3+} to rigidify the outer leaflet of the liposome. We therefore examined the effect of Pr^{3+} on anisotropy of the external leaflet of liposomes in the presence of 200 mM of solutes being examined. DPPC liposomes were incubated with the fluorescent phospholipid analogue and anisotropy probe, DPH-HPC [2-(3-(diphyenylhexatrienyl)propanyl)-1-hexadecanyl-*sn*-glycero-3-phosphocholine] to "label" the outer (exofacial) leaflet of the membrane for fluidity measurements (Negrete et al., 1996b). Liposomes incubated in buffer containing 200 mM permeant solute for 30 min had anisotropy measured as a function of temperature. Fig. 1 A shows the effect of increasing temperature on the anisotropy of the exofacial leaflet of the bilayer in the presence or absence of 10 mM Pr^{3+} and in the presence of 200 mM glycerol. Between 24° and 34°C, there is little change in the anisotropy of the
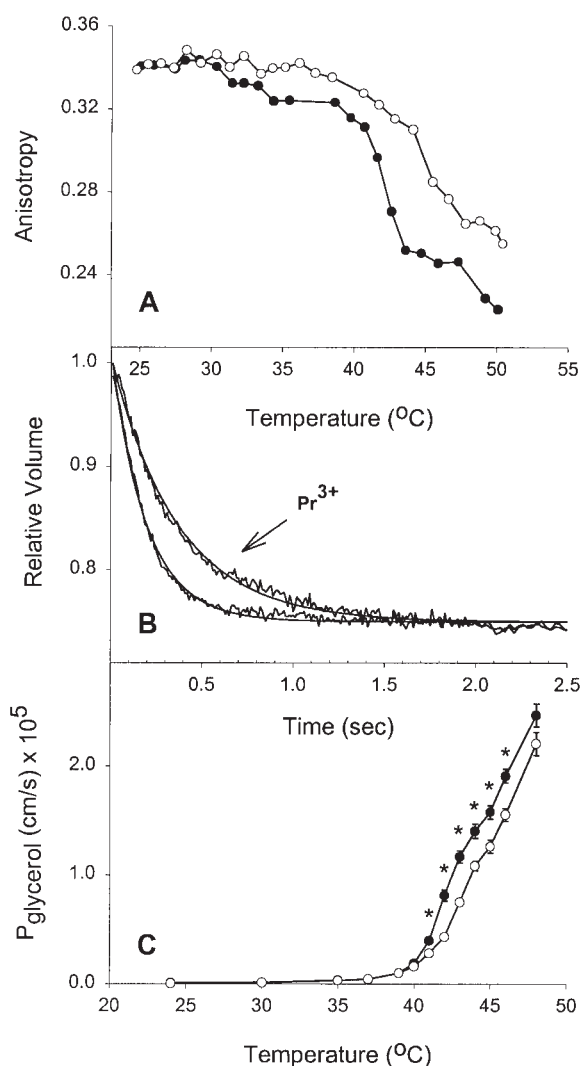

Figure 1. Effect of rigidifying a single leaflet on glycerol permeability. (A) Effect of extravesicular Pr^{3+} on bilayer fluidity at different temperatures. DPPC liposomes were incubated in 1 mM DPH-HPC, and then loaded with 200 mM glycerol before performing anisotropy measurements at different temperatures. (●) Control liposomes, (○) liposomes treated with 10 mM Pr^{3+}. (B) Stopped-flow experiments on control and Pr^{3+}-treated vesicles showing glycerol flux through liposomes at 42°C. Averaged time courses and fitted single exponential curves are shown. (C) Effect of extravesicular Pr^{3+} on glycerol permeability at different temperatures. Results shown are from four separate liposome preparations (mean ± SEM). Where error bars are not visible, the symbol is wider than the error. (●) Control DPPC liposomes, (○) the Pr^{3+}-treated liposomes. *$P < 0.05$ by t test.

membrane and no difference between Pr^{3+} and control liposomes. However, above 39°C, there is a sharp decrease in anisotropy that corresponds to a dramatic increase in leaflet fluidity at or near the phase-transition temperature (T_c) of the leaflet. In the presence of exofacially bound Pr^{3+}, however, the acyl chains are rigidified and as a consequence the increase in fluidity occurs 2–3°C higher. Consistent with previous studies, this

indicates that Pr^{3+} binding has increased T_c for the exofacial leaflet (Hunt and Tipping, 1978; Schmidt et al., 1978; Sillerud and Barnett, 1982). Stopped-flow experiments in which CF and glycerol-loaded liposomes were rapidly exposed to a glycerol gradient defined the glycerol permeabilities of both native and Pr^{3+}-treated liposomes (Fig. 1 B). Upon exposure to the gradient, glycerol efflux from liposomes results in the formation of an immediate osmotic gradient for water. Water then exits the liposomes resulting in vesicle shrinkage and self-quenching of entrapped CF. The superposition of glycerol efflux from native and Pr^{3+}-treated vesicles at 42°C reveals that the rate of shrinkage and hence the permeability is reduced when Pr^{3+} is present in the exofacial leaflet. Combined glycerol permeabilities as a function of temperature are shown in Fig. 1 C. Solute permeability was found to increase dramatically above 40°C. With the addition of 10 mM Pr^{3+}, glycerol permeabilities were significantly lower at temperatures above 40°C ($P < 0.05$ where indicated by asterisks), thus demonstrating that rigidifying one leaflet of the bilayer was sufficient to reduce the overall permeability of the membrane to this nonelectrolyte.

Glycerol ($M_r = 92.09$) has a relatively large molecular volume. Therefore, we tested three other uncharged solutes of varying molecular weight to ascertain whether inducing bilayer asymmetry with Pr^{3+} would result in reduced permeability for other nonelectrolytes. In panel A, Figs. 2–4, it can be noted that addition of Pr^{3+} to formamide ($M_r = 45.04$), acetamide ($M_r = 59.07$), and urea ($M_r = 60.06$) equilibrated liposomes, respectively, resulted in a reduction in fluidity of the exofacial leaflet in a manner similar to what is observed in the presence of glycerol. Therefore, the nature of the solute did not alter the interaction with Pr^{3+} or its effect on the membrane. Panel B, Figs. 2–4, shows representative tracings of stopped-flow experiments carried out above 40°C in the presence or absence of Pr^{3+}. These demonstrate a reduction in solute permeability as judged by the initial rate of shrinkage for each solute. Combined permeability data for each solute is shown as a function of temperature (Panel C, Figs. 2–4). Each shows a significantly lowered permeability above T_c when fluidity is reduced by Pr^{3+}. It is clear that reducing acyl chain fluidity in a single leaflet is sufficient to alter the permeability of the entire membrane to multiple small nonelectrolytes.

Water and solutes appear to obey the solubility-diffusion model for permeation across a bilayer. However, less information is available on the mechanisms of permeation of gases and protons. Fig. 5 shows the results of proton permeability experiments on DPPC liposomes over a range of temperatures. Fig. 5 A shows two experiments in which liposomes were rapidly exposed to a pH gradient (pH 7.50 inside/7.06 outside). The
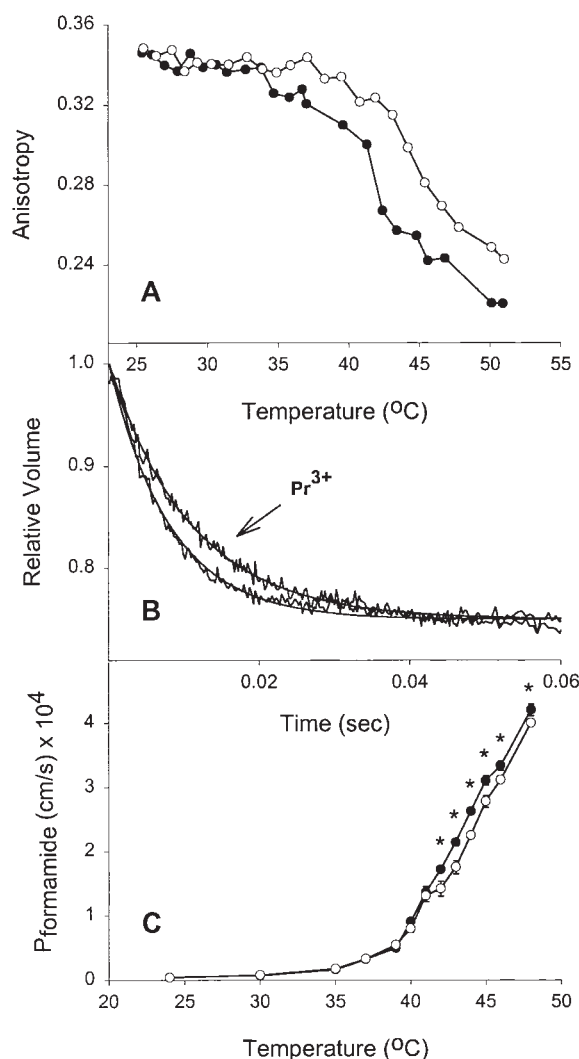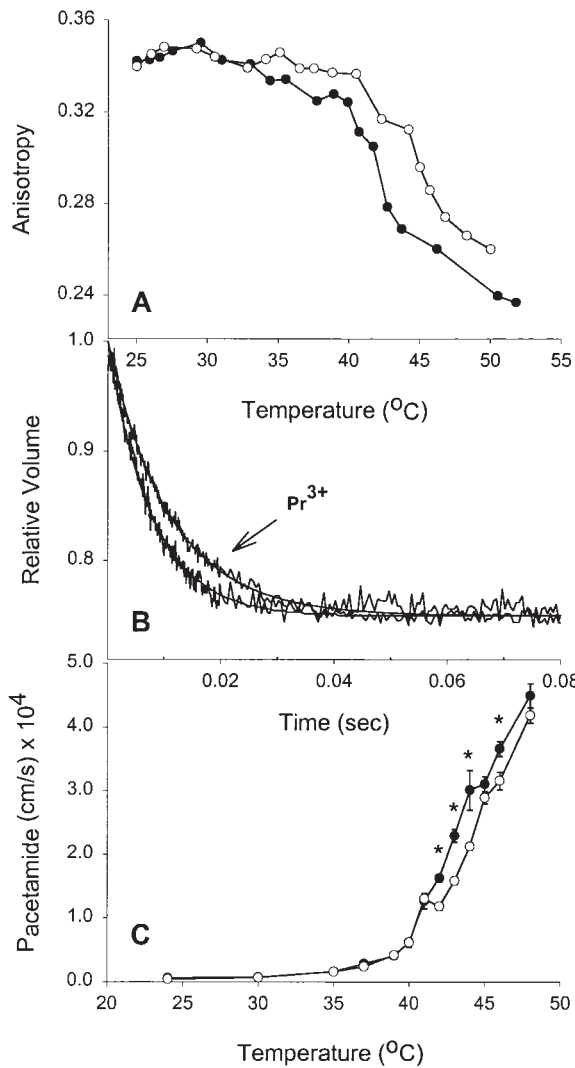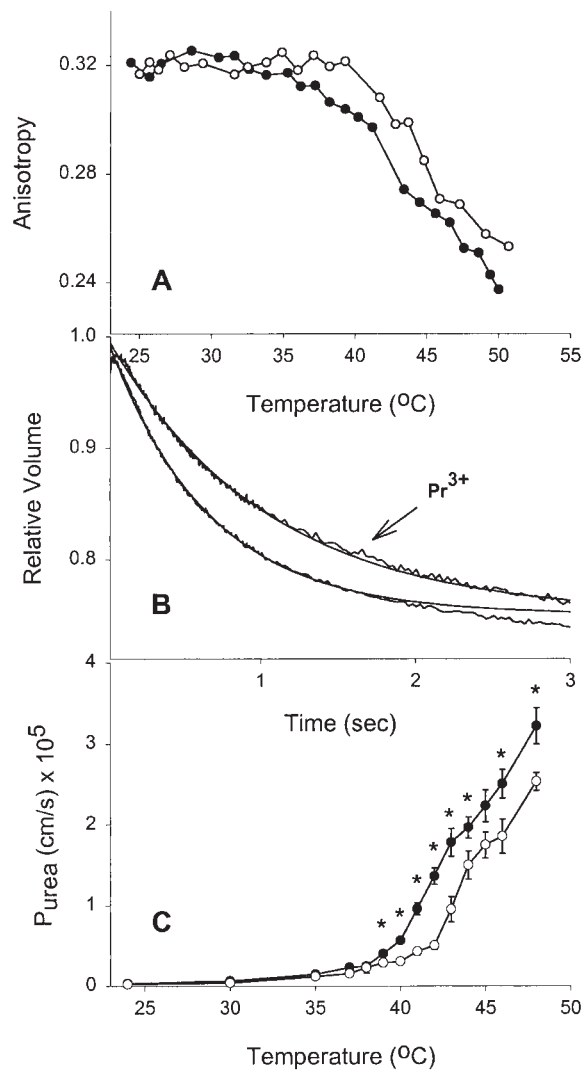

Figure 2. Effect of rigidifying a single leaflet on formamide permeability. (A) Effect of extravesicular Pr^{3+} on bilayer fluidity at different temperatures. DPPC liposomes were incubated in 1 mM DPH-HPC, and then loaded with 200 mM formamide before performing anisotropy measurements at different temperatures. (●) Control liposomes, (○) liposomes treated with 10 mM Pr^{3+}. (B) Stopped-flow experiments on control and Pr^{3+}-treated vesicles showing formamide flux through liposomes at 43°C. Averaged time courses and fitted single exponential curves are shown. (C) Effect of extravesicular Pr^{3+} on formamide permeability at different temperatures. Results shown are from four separate liposome preparations (mean ± SEM). Where error bars are not visible, the symbol is wider than the error. (●) Control DPPC liposomes, (○) the Pr^{3+}-treated liposomes. $*P < 0.05$ by t test.

pH-dependent quenching of entrapped CF illustrates the reduction in acidification rate at 48°C when Pr^{3+} is present. Fig. 5 B shows H^+ permeability as a function of temperature. There is a noticeable increase in proton permeability above T_c; however, at 48°C it is only fourfold higher than baseline levels. This is compared with 129 ± 36-fold (SEM) increases at 48°C for the four

Figure 3. Effect of rigidifying a single leaflet on acetamide permeability. (A) Effect of extravesicular Pr^{3+} on bilayer fluidity at different temperatures. DPPC liposomes were incubated in 1 mM DPH-HPC, and then loaded with 200 mM acetamide before performing anisotropy measurements at different temperatures. (●) Control liposomes, (○) liposomes treated with 10 mM Pr^{3+}. (B) Stopped-flow experiments on control and Pr^{3+}-treated vesicles showing acetamide flux through liposomes at 43°C. Averaged time courses and fitted single exponential curves are shown. (C) Effect of extravesicular Pr^{3+} on acetamide permeability at different temperatures. Results shown are from four separate liposome preparations (mean ± SEM). Where error bars are not visible, the symbol is wider than the error. (●) Control DPPC liposomes, (○) the Pr^{3+}-treated liposomes. *$P < 0.05$ by t test.

Figure 4. Effect of rigidifying a single leaflet on urea permeability. (A) Effect of extravesicular Pr^{3+} on bilayer fluidity at different temperatures. DPPC liposomes were incubated in 1 mM DPH-HPC, and then loaded with 200 mM urea before performing anisotropy measurements at different temperatures. (●) Control liposomes, (○) liposomes treated with 10 mM Pr^{3+}. (B) Stopped-flow experiments on control and Pr^{3+}-treated vesicles showing urea flux through liposomes at 42°C. Averaged time courses and fitted single exponential curves are shown. (C) Effect of extravesicular Pr^{3+} on urea permeability at different temperatures. Results shown are from four separate liposome preparations (mean ± SEM). Where error bars are not visible, the symbol is wider than the error. (●) Control DPPC liposomes, (○) the Pr^{3+}-treated liposomes. *$P < 0.05$ by t test.

small nonelectrolytes tested in this study. Therefore, dramatically increasing bilayer fluidity at temperatures above T_c only results in modest increases in the ability of protons to cross the bilayer. Rigidification of the exofacial leaflet with Pr^{3+} completely abolishes the phase-transition–induced permeability increase seen in native vesicles. These data argue that proton permeability is only weakly correlated with membrane fluidity.
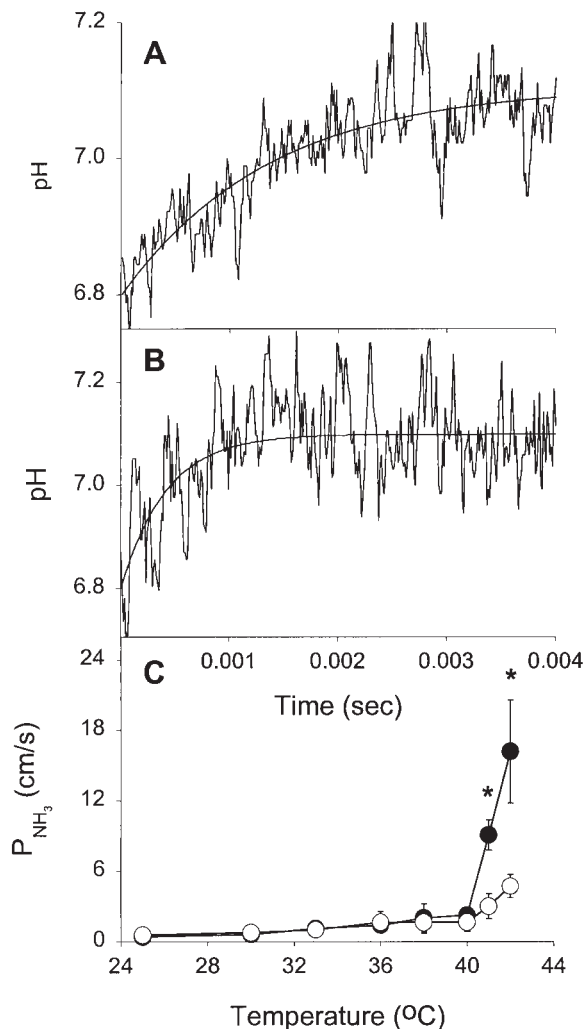
NH_3 and CO_2 diffuse rapidly across cell membranes, and NH_3 permeation is thought to occur by solubility diffusion. We examined the transport properties of both gases across DPPC liposomes and examined the influence of temperature and bilayer asymmetry on the process. Fig. 6, A and B, shows the permeation of NH_3 into DPPC liposomes at 42°C in the presence and ab-
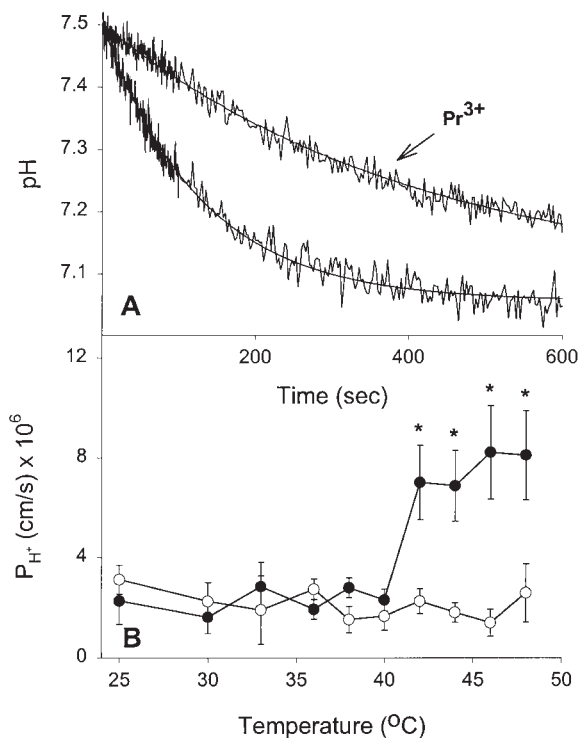
Figure 5. Effect of extravesicular Pr^{3+} on proton permeability at different temperatures. (A) Stopped-flow experiments on control and Pr^{3+}-treated vesicles showing proton flux through liposomes at 48°C. Time courses and fitted single exponential curves are shown. (B) Proton permeabilities as a function of temperature. Results shown are from four separate liposome preparations (mean ± SEM). (●) Control DPPC liposomes, (○) the Pr^{3+}-treated liposomes. *$P < 0.05$ by t test.

Figure 6. Effect of extravesicular Pr^{3+} and temperature on NH_3 flux. (A) Stopped-flow experiments on Pr^{3+}-treated vesicles showing NH_3 flux through liposomes at 42°C. Averaged time course and fitted single exponential curve are shown. (B) Stopped-flow experiments on control vesicles showing NH_3 flux through liposomes at 42°C. Averaged time course and fitted single exponential curve are shown. (C) Effect of extravesicular Pr^{3+} on proton permeability at different temperatures. Results shown are from four separate liposome preparations (mean ± SEM). (●) Control DPPC liposomes, (○) the Pr^{3+}-treated liposomes. *$P < 0.05$ by t test.

sence, respectively, of Pr^{3+}. The rate of permeation is slower when the exofacial leaflet is rigidified (Fig. 6 A). Of note is the extreme rapidity of this process, which is complete within 4 ms. The temperature dependence of NH_3 permeation is shown in Fig. 6 C. At 25°C, the permeability coefficient is ~0.4 cm/s, compared with 4×10^{-6} cm/s for formamide (the fastest of the solutes). Permeability rapidly increased above 40°C, indicating that fluidity is a major determinant in the rate of NH_3 permeation across phospholipid bilayers. At temperatures higher than 42°C, NH_3 permeation in response to the applied NH_3 gradient was complete within the dead time of the instrument (~0.7 ms), and therefore unmeasurable. Rigidification of the exofacial leaflet resulted in a marked reduction in the permeability of the membrane to NH_3 at temperatures above T_c. This suggests that NH_3, like water and solutes, crosses biological membranes by a solubility-diffusion mechanism.

A CO_2 permeability assay recently developed in our laboratory measures the acidification occurring within liposomes after exposure to a CO_2 gradient that is supplied in the form of a CO_2/HCO_3^- solution (Prasad et al., 1998). Upon diffusion across the bilayer, CO_2 is hy-

drated to carbonic acid, which subsequently dissociates to bicarbonate ion and a proton. The presence of entrapped carbonic anhydrase within the liposome ensures that the hydration reaction is not rate limiting, but that gas permeation is. When the CO_2 permeability of DPPC liposomes was measured, it was found to be independent of temperature (Fig. 7). Fig. 7 A illustrates the equivalence of CO_2-dependent acidification rates in liposomes at 25° and 45°C from stopped-flow experiments. Fig. 7 B shows the lack of effect of temperature on the calculated CO_2 permeability coefficients. This was in dramatic contrast to the response of NH_3 to elevated temperature and
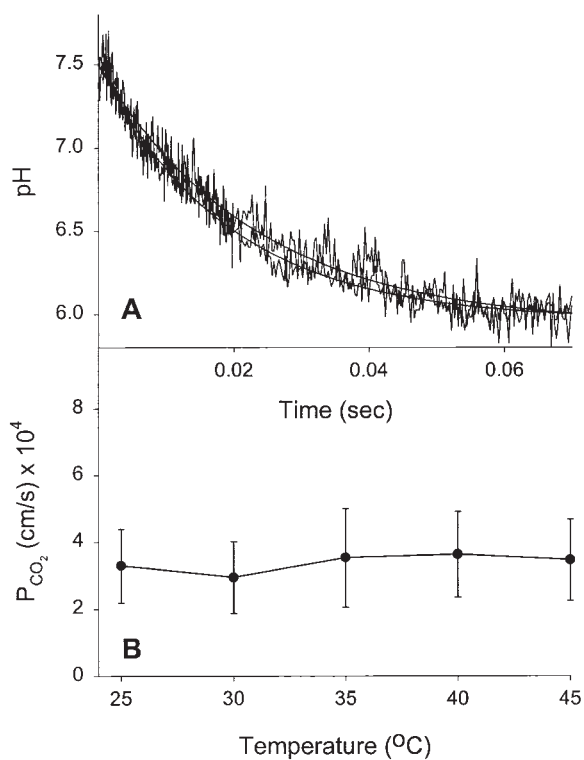
Figure 7. Effect of temperature on CO_2 flux. (A) Stopped-flow experiments on DPPC liposomes showing equivalence of CO_2 flux rates at 25° and 45°C. Averaged time courses and fitted single exponential curves are shown. (B) CO_2 permeabilities as a function of temperature. Results shown are from four separate liposome preparations (mean ± SEM).

strongly implies that fluidity does not influence the ability of CO_2 to cross a model phospholipid bilayer. Even at temperatures well above T_c, there was no effect on CO_2 permeability. This data suggests that in a biological context, lipid bilayer asymmetry or phospholipid composition play no role in either limiting or facilitating the transfer of CO_2 between body compartments.

discussion

The rare earth metal Pr^{3+} has been used as a nuclear magnetic resonance shift reagent to discriminate between the inner and outer choline methyl resonances of dimyristoylphosphatidylcholine liposomes (Sillerud and Barnett, 1982). Addition of Pr^{3+} to liposomes increased the gel to liquid-crystalline phase-transition temperature of just the outer leaflet by several degrees. Significantly, this implied that the coupling of both halves of a phospholipid bilayer is sufficiently weak that each leaflet can undergo a thermotropic phase-transition independently. Pr^{3+} binding was shown to exert this effect by reducing the fluidity of the outer leaflet of DPPC liposomes (Negrete et al., 1996b). It appears likely that the Pr^{3+} binds to multiple phosphate head groups, reducing their mobility and thereby the mobil-

ity of their attached hydrocarbon chains. Negrete et al. (1996b) demonstrated that binding to the phospholipid head group stabilized and rigidified the leaflet, and this was reflected in a decrease in water permeability at temperatures above T_c. In this study, we further exploited the hemi-bilayer rigidifying properties of Pr^{3+} to examine the effect of inducing bilayer asymmetry on solute, proton, and gas fluxes in an effort to better understand their permeation properties.

DPPC has been used extensively as a model lipid to explore the behavior of phospholipid bilayers and is therefore well characterized. The advantages of using DPPC in these experiments were the phosphorylcholine head groups necessary for Pr^{3+} binding, and its high T_c, which allows an exploration of permeant behavior in both the gel and liquid-crystal states. As most PCs have a very low T_c and exist in cell membranes only in the liquid-crystal phase, they don't allow an exploration of membrane permeant behavior in asymmetric bilayers at temperatures above and below T_c.

In a series of solute flux experiments, we initially sought to determine whether Pr^{3+} would reduce the fluidity of the outer leaflet in liposomes that were loaded with high concentrations of solute (200 mM). Panel A, Figs. 1–4, demonstrates that there was no observable difference on membrane fluidity in the presence or absence of Pr^{3+} as measured by fluorescence polarization anisotropy between 24° and 35°C. The control liposomes exhibited a steep decrease in anisotropy when temperatures were raised higher than 39°C, which indicated dramatic increases in membrane fluidity as a result of the membrane phase transition from a gel to liquid-crystalline state. When Pr^{3+} was added, the thermotropic phase-transition occurred 1°–3°C higher. This demonstrated that high concentrations of solute were not affecting Pr^{3+} binding or its influence as a stabilizing reagent on the outer leaflet. The permeability of DPPC membranes to glycerol, formamide, acetamide, and urea were tested over a range of temperatures (panel C, Figs. 1–4) and the effect of membrane phase transition on permeability was striking, with permeabilities above baseline (i.e., 24°C) of 235-, 99-, 74-, and 106-fold for glycerol, formamide, acetamide, and urea, respectively. This is consistent with the high degree of disorder that prevails in the liquid-crystal state. Phase transition is associated with a conformational change in the acyl chains from a predominantly straight (trans) conformation to the gauche conformation, which occurs due to C–C bond rotation. This results in an expansion of the area occupied by the chains and a concomitant reduction in the thickness of the bilayer (New, 1997). At temperatures below 39°C, Pr^{3+} had no influence on membrane permeability to any of the solutes. However, at 41°–42°C, there was a significantly decreased permeability due to outer leaflet rigidification.

These data confirmed that membrane fluidity was a rate-limiting factor for nonelectrolyte permeability, and, more significantly, that reducing the fluidity of a single leaflet is sufficient to significantly retard the passage of small uncharged molecules. Each leaflet in the bilayer therefore appears to exert an independent resistance to the passage of solutes, with the overall permeability a function of the sum of the resistances exerted by two leaflets. This relationship has previously been found to apply to water permeability (Negrete et al., 1996b) and may be expressed as:

$$1/P_{ab} = 1/P_a + 1/P_b, \qquad (7)$$

where P_{ab} is the permeability of the membrane, P_a is the permeability of leaflet a and P_b is the permeability of leaflet b. To test whether this relationship accurately predicts the solute permeability behavior of Pr^{3+}-rigidified liposomes, we calculated asymmetric bilayer permeabilities. At temperatures above T_c, we know the temperatures at which anisotropies of native and Pr^{3+}-treated liposomes are the same (panel A, Figs. 1–4); e.g., in Fig. 3 A the anisotropy of the Pr^{3+}-treated leaflet at 44°C has the same value as the control leaflet at 41°C. For identical fluidities, we assume identical permeabilities (Lande et al., 1995) and in this way derive a permeability value for a Pr^{3+}-treated leaflet. From Fig. 3 C for acetamide, for example:

$$P_{acet.}[DPPC bilayer]_{41°C} = 1.266 \times 10^{-4} \text{ cm/s}$$

$$\Rightarrow P_{acet.}[DPPC leaflet]_{41°C} = 2.532 \times 10^{-4} \text{ cm/s}$$

$$= P_{acet.}[Pr^{3+}\text{-}DPPC leaflet]_{44°C}.$$

(from Eq. 7)

We now calculate a DPPC leaflet permeability at 44°C from the experimentally determined value for control liposomes.

$$P_{acet.}[DPPC bilayer]_{44°C} = 3.012 \times 10^{-4} \text{ cm/s}$$

$$\Rightarrow P_{acet.}[DPPC leaflet]_{44°C} = 6.024 \times 10^{-4} \text{ cm/s}.$$

(from Eq. 7)

Having now derived values for the acetamide permeability of a DPPC leaflet and a Pr^{3+}-DPPC leaflet at 44°C, we can add their reciprocals to arrive at a predicted Pr^{3+}-treated membrane permeability of 1.78×10^{-4} cm/s. This compares favorably with the experimentally measured value of $2.12 \pm 0.06 \times 10^{-4}$ cm/s.

Predicted values compared with those measured for the other solutes were 1.08×10^{-5} vs. 1.26×10^{-5} cm/s for glycerol, 2.21×10^{-4} vs. 2.78×10^{-4} cm/s for formamide, and 8.58×10^{-6} vs. 9.55×10^{-6} cm/s for urea. This close concordance of measured and predicted permeabilities for asymmetric membranes strongly supports the model of leaflets offering independent resistances to solute permeation. Bilayer asymmetry is therefore a plausible mechanism by which epithelial cells may limit the permeation of solutes such as urea.

The permeability of water, solutes, and NH_3 have been found to correlate strongly with membrane fluidity; however, proton permeability correlates only weakly (Lande et al., 1995; Wilkes et al., 1989). Although protons are ions, they traverse membranes at rates several orders of magnitude higher than alkali or halide ions (Finkelstein, 1987). The fluidity dependence of H^+ permeability in DPPC liposomes can be seen in Fig. 5 B. In contrast to the massive increase in solute permeability upon phase transition of the liposomal membrane (approximately two orders of magnitude), H^+ permeability increased only fourfold. Rigidifying the outer leaflet eliminated that modest increase. Proton permeation has been postulated to occur by a pathway distinct from that of water and solutes. Two prevailing hypotheses as to the nature of that pathway are that protons can be shuttled from one side of the membrane to the other by virtue of hydrogen-bonded "water wires" embedded in the hydrocarbon (Nagle and Morowitz, 1978; Pomes and Roux, 1996). Alternatively, weak acids present as "contaminants" in the bilayer may act as proton carriers (Gutknecht, 1987a,b). According to the weak-acid hypothesis, protons cross the membrane in a non-ionic form (HA), and upon proton release the carrier must translocate back as an anion (A^-). This process may be driven either by voltage or pH gradients, but it is thought that A^- translocation is the rate-limiting step. Our data confirms the weak dependence of proton transfer on fluidity; however, the effect of Pr^{3+} in dramatically reducing permeability was unexpected and may not necessarily be due to its actions as a leaflet fluidity-reducing reagent. Other potential explanations are the possibility that externally bound Pr^{3+} somehow blocks access to internal water molecules that constitute water wires, or that Pr^{3+} is inhibiting access to, or freedom of movement of, the weak acid proton carrier. The experimental methodology employed doesn't allow us to discriminate between these possibilities, but the results do add to the growing body of evidence suggesting that protons cross phospholipid bilayers by a mechanism that is independent of the water and solute pathway. Mobility of the hydrocarbon chains does not appear to be as important. As such, bilayer asymmetry is unlikely to play a major role in providing a barrier to acid flux. Indeed, Bhaskar et al. (1992) have shown that gastric mucus may be the predominant barrier to proton flux in the stomach.

NH_3 is a neutral lipophilic molecule that is freely diffusible across most cell membranes. Notable exceptions have been described, however, in the medullary

thick ascending limb of Henle (Kikeri et al., 1989), colonic crypts (Singh et al., 1995), and rabbit urinary bladder epithelium (Chang et al., 1994). In all cases, the apical membrane was shown to be virtually impermeable to NH_3, whilst the basolateral membrane presented no significant barrier to NH_3 transport. In the case of the thick ascending limb of Henle, low surface area of the apical membrane plays a critical role in its barrier properties. Our data clearly show that NH_3 permeability in DPPC liposomes is strongly influenced by membrane fluidity. Induction of a membrane asymmetry significantly restricts NH_3 permeability at temperatures above T_c. This data confirms the nature of NH_3 flux that occurs by a solubility-diffusion mechanism and demonstrates the efficacy of reducing outer leaflet fluidity in reducing overall permeability to this gas. We conclude that an alteration to lipid structure in a single leaflet, such as is seen with the apical membranes of barrier epithelia, is sufficient to reduce NH_3 permeability. This implies that each leaflet offers an independent resistance to NH_3 flux.

The system we have used to create bilayer asymmetry allows us to demonstrate the effect of a single leaflet rigidification on the permeation behavior of a range of biologically relevant molecules. These features are applicable to real cell membranes that, it should be noted, exist physiologically in the liquid-crystal rather than the gel state; i.e., in a state analogous to DPPC membranes at temperatures above 41°C. These results clearly demonstrate that epithelial cells with a requirement to restrict diffusional processes; e.g., in the thick ascending limb or collecting duct of the kidney, can do so by means of erecting apical membranes with asymmetric leaflet fluidities.

Gastric glands, which contain parietal and chief cells, are the only epithelia described that possess a barrier to CO_2 permeation (Walsbren et al., 1994). In addition, since urine and possibly collecting duct P_{CO2} can reach 80 mmHg while blood P_{CO2} is 40 mmHg, it is highly likely that mammalian bladder also exhibits low permeability to CO_2. CO_2, like NH_3, is readily permeable to most lipid membranes (Gutknecht et al., 1977). However, because CO_2 permeates most membranes extremely rapidly, the mechanism by which it crosses membranes has not been studied. We recently developed a technique for measuring the CO_2 flux into liposomes (Prasad et al., 1998) and used it to examine the influence of membrane fluidity on CO_2 permeation. Unexpectedly, there was no change in permeability when liposomes underwent the gel to liquid-crystal phase transition at 40–41°C (Fig. 7 B). This suggests that CO_2 transport across membranes is not governed by a solubility-diffusion mechanism. Prasad et al. (1998) demonstrated that liposomes of varying lipid composition with a range of membrane fluidities could substantially alter water permeability, while having no effect on CO_2 permeability. We conclude therefore that gastric gland cells and possibly the urinary bladder and renal cortex as well, maintain lumenal CO_2 gradients with respect to interstitium by mechanisms that do not primarily depend on apical membrane bilayer asymmetry and fluidity reduction in the exofacial leaflet.

These results demonstrate that for molecules that permeate across membranes by a solubility-diffusion mechanism, reducing the fluidity of a single leaflet of the bilayer is sufficient to reduce permeability. This finding has implications for our understanding of permeation processes in that it allows us to treat the resistance to permeation offered by each leaflet as an independent parameter. Therefore, the permeability properties of the bilayer are not some amalgam or synergy of the activities of each leaflet, but are independent and additive in their own right. The bilayer can be considered, much like an electrical circuit, as a pair of resistors in series for the permeation of solutes, NH_3 and water (Negrete et al., 1996b).

CO_2 permeability was shown not to occur by a solubility-diffusion pathway as its rate of passage across the liposomal membrane was completely independent of temperature and membrane fluidity. It is likely that these unusual properties are due to its molecular linearity and lack of any permanent dipole moment. Simon and Gutknecht (1980) demonstrated that CO_2 could dissolve into a number of organic solvents as well as into an egg lecithin bilayer with only small differences in the partition coefficient. Addition of cholesterol to the egg lecithin, which would have resulted in reduced membrane fluidity, had only a minor effect on the partition coefficient (Simon and Gutknecht, 1980). Prasad et al. (1998) have recently shown that liposomes of widely varying fluidity have identical CO_2 flux rates. Therefore, neither solubility nor diffusion of CO_2 appears to be affected by lipid composition or lipid packing. To date, only the gastric gland has been directly shown to present a barrier to CO_2 diffusion (Walsbren et al., 1994); however, the study did not investigate mechanisms for this remarkable property. Based on the results presented here, we conclude that it is unlikely to be the lipid composition of these cells that presents the barrier. In particular, our results suggest that proteins inserted in, or associated with, the membrane determine the membrane's permeability to CO_2

413   Hill et al.

r e f e r e n c e s

Bhaskar, K.R., P. Garik, B.S. Turner, J.D. Bradley, R. Bansil, H.E. Stanley, and J.T. LaMont. 1992. Viscous fingering of HCl through gastric mucin. *Nature.* 360:458–461.

Chang, A., T.G. Hammond, T.T. Sun, and M.L. Zeidel. 1994. Permeability properties of the mammalian bladder apical membrane. *Am. J. Physiol.* 267:C1483–C1492.

Disalvo, E.A. 1988. Permeability of water and polar solutes in lipid bilayers. *Adv. Colloid Interface Sci.* 29:141–170.

Finkelstein, A. 1987. Water Movement Through Lipid Bilayers, Pores, and Plasma Membranes: Theory and Reality. John Wiley & Sons-Interscience, New York, NY. 93–151.

Giocondi, M.C., and C. Le Grimellec. 1991. Water permeation in Madin-Darby canine kidney cells is modulated by membrane fluidity. *Biochim. Biophys. Acta.* 1064:315–320.

Grossman, E.B., H.W. Harris, Jr., R.A. Star, and M.L. Zeidel. 1992. Water and nonelectrolyte permeabilities of apical membranes of toad urinary bladder granular cells. *Am. J. Physiol.* 262:C1109–C1118.

Gutknecht, J. 1987a. Proton conductance through phospholipid bilayers: water wires or weak acids? *J. Bioenerg. Biomembr.* 19:427–442.

Gutknecht, J. 1987b. Proton/hydroxide conductance and permeability through phospholipid bilayer membranes. *Proc. Natl. Acad. Sci. USA.* 84:6443–6446.

Gutknecht, J., M.A. Bisson, and F.C. Tosteson. 1977. Diffusion of carbon dioxide through lipid bilayer membranes. Effects of carbonic anhydrase, bicarbonate, and unstirred layers. *J. Gen. Physiol.* 69:779–794.

Hunt, G.R, and L.R. Tipping. 1978. A H NMR study of the effects of metal ions, cholesterol and n-alkanes on phase transitions in the inner and outer monolayers of phospholipid vesicular membranes. *Biochim. Biophys. Acta.* 507:242–261.

Kikeri, D., A. Sun, M.L. Zeidel, and S.C. Hebert. 1989. Cell membranes impermeable to NH_3. *Nature.* 339:478–480.

Lande, M.B., J.M. Donovan, and M.L. Zeidel. 1995. The relationship between membrane fluidity and permeabilities to water, solutes, ammonia, and protons. *J. Gen. Physiol.* 106:67–84.

Lande, M.B., N.A. Priver, and M.L. Zeidel. 1994. Determinants of apical membrane permeabilities of barrier epithelia. *Am. J. Physiol.* 267:C367–C374.

Nagle, J.F, and H.J. Morowitz. 1978. Molecular mechanisms for proton transport in membranes. *Proc. Natl. Acad. Sci. USA.* 75:298–302.

Negrete, H.O., J.P. Lavelle, J. Berg, S.A. Lewis, and M.L. Zeidel. 1996a. Permeability properties of the intact mammalian bladder epithelium. *Am. J. Physiol.* 271:F886–F894.

Negrete, H.O., R.L. Rivers, A.H. Goughs, M. Colombini, and M.L. Zeidel. 1996b. Individual leaflets of a membrane bilayer can independently regulate permeability. *J. Biol. Chem.* 271:11627–11630.

New, R.R.C. 1997. Introduction. *In* Liposomes: A Practical Approach. R.R.C. New, editor. Oxford University Press, New York, NY. 1–32.

Overton, E. 1899. Ueber die allgemeinen osmotischen Eigenschaften der Zelle, ihre vermutlichen Ursachen und ihre Bedeutung fur die Physiologie. *Vierteljahrsschr. Naturforsch. Ges. Zuerich.* 44:88–135.

Paula, S., A.G. Volkov, A.N. Van Hoek, T.H. Haines, and D.W. Deamer. 1996. Permeation of protons, potassium ions, and small polar molecules through phospholipid bilayers as a function of membrane thickness. *Biophys. J.* 70:339–348.

Pomes, R., and B. Roux. 1996. Structure and dynamics of a proton wire: a theoretical study of H^+ translocation along the single-file water chain in the gramicidin A channel. *Biophys. J.* 71:19–39.

Prasad, G.V.R., L.A. Coury, F. Finn, and M.L. Zeidel. 1998. Reconstituted aquaporin 1 water channels transport CO_2 across membranes. *J. Biol. Chem.* 273:33123–33126.

Priver, N.A., E.C. Rabon, and M.L. Zeidel. 1993. Apical membrane of the gastric parietal cell: water, proton, and nonelectrolyte permeabilities. *Biochemistry.* 32:2459–2468.

Rivers, R., A. Blanchard, D. Eladari, F. Leviel, M. Paillard, R.A. Podevin, and M.L. Zeidel. 1998. Water and solute permeabilities of medullary thick ascending limb apical and basolateral membranes. *Am. J. Physiol.* 274:F453–F462.

Schmidt, C.F., Y. Barenholz, C. Huang, and T.E. Thompson. 1978. Monolayer coupling in sphingomyelin bilayer systems. *Nature.* 271:775–777.

Sillerud, L.O., and R.E. Barnett. 1982. Lack of transbilayer coupling in phase transitions of phosphatidylcholine vesicles. *Biochemistry.* 21:1756–1760.

Simon, S.A., and J. Gutknecht. 1980. Solubility of carbon dioxide in lipid bilayer membranes and organic solvents. *Biochim. Biophys. Acta.* 596:352–358.

Simons, K., and G. van Meer. 1988. Lipid sorting in epithelial cells. *Biochemistry.* 27:6197–6202.

Singh, S.K., H.J. Binder, J.P. Geibel, and W.F. Boron. 1995. An apical permeability barrier to NH_3/NH_4^+ in isolated, perfused colonic crypts. *Proc. Natl. Acad. Sci. USA.* 92:11573–11577.

van Meer, G. 1989. Lipid traffic in animal cells. *Annu. Rev. Cell Biol.* 5:247–275.

van Meer, G., and K. Simons. 1986. The function of tight junctions in maintaining differences in lipid composition between the apical and basolateral cell surface domains of MDCK cells. *EMBO (Eur. Mol. Biol. Organ.) J.* 5:1455–1464.

Verkman, A.S., and S.K. Masur. 1988. Very low osmotic water permeability and membrane fluidity in isolated toad bladder granules. *J. Membr. Biol.* 104:241–251.

Walsbren, S.J., J.P. Geibel, I.M. Modlin, and W.F. Boron. 1994. Unusual permeability properties of gastric gland cells. *Nature.* 368:332–335.

Walter, A., and J. Gutknecht. 1986. Permeability of small nonelectrolytes through lipid bilayer membranes. *J. Membr. Biol.* 90:207–217.

Wilkes, J.M., H.J. Ballard, D.T. Dryden, and B.H. Hirst. 1989. Proton permeability and lipid dynamics of gastric and duodenal apical membrane vesicles. *Am. J. Physiol.* 256:G553–G562.

Worman, H.J., T.A. Brasitus, P.K. Dudeja, H.A. Fozzard, and M. Field. 1986. Relationship between lipid fluidity and water permeability of bovine tracheal epithelial cell apical membranes. *Biochemistry.* 25:1549–1555.

Zachowski, A., E. Favre, S. Cribier, P. Herve, and P.F. Devaux. 1986. Outside–inside translocation of aminophospholipids in the human erythrocyte membrane is mediated by a specific enzyme. *Biochemistry.* 25:2585–2590.

Zachowski, A., J.-P. Henry, and P.F. Devaux. 1989. Control of transmembrane lipid asymmetry in chromaffin granules by an ATP-dependent protein. *Nature.* 340:75–76.

Zeidel, M.L. 1996. Low permeabilities of apical membranes of barrier epithelia: what makes watertight membranes watertight? *Am. J. Physiol.* 271:F243–F245.